JOURNAL OF MATERIALS SCIENCE: MATERIALS IN MEDICINE 5 (1994) 263–268

Shape change and phase transition of needle-like non-stoichiometric apatite crystals

L. YUBAO*‡, C.P.A.T. KLEIN‡, J. DE WIJN‡, S. VAN DE MEER‡, K. DE GROOT‡

‡*Department of Biomaterials, University of Leiden, Rijnsburgerweg 10, bld. 55, 2333 AA Leiden, The Netherlands* * *Institute of Materials Science and Technology, Sichuan University, Chengdu 610064, People's Republic of China*

Nanometre-size needle-like non-stoichiometric apatite crystals are made in our laboratory by hydrothermal treatment at 140 °C at a pressure of 0.3 MPa for 2 h. The shape change and phase transition of these crystals are studied using transmission electron microscopy (TEM), X-ray diffractometer (XRD) and infrared spectroscopy (IR). The results show that water molecules are present in the crystal structure of non-stoichiometric apatite. The condensation of HPO_4^{2-} ions can happen over a wide temperature range more than 600 °C and is followed closely by the reaction of $P_2O_7^{4-}$ ions with OH^- ions. The obvious TCP phase at 750 °C is the outcome of the fusion and recrystallization of the needle-like crystals at 650 °C and 750 °C. Generally, stoichiometric apatite cannot contain water in its crystal structure while non-stoichiometric apatite can. Maybe this is the reason why bone contains non-stoichiometric apatite.

1. Introduction

Hydroxyapatite (HA), $Ca_{10}(PO_4)_6(OH)_2$, and tricalcium phosphate (TCP), $Ca_3(PO_4)_2$, are two main calcium phosphate salts which have been studied extensively and used clinically [1–5]. It is known that the mineral constituent of human hard tissues generally shows a porous biphasic (HA + TCP) structure after sintering at high temperature. Probably due to the analogy to bone mineral, artificially sintered porous biphasic or multiphasic (HA + α- or/and β-TCP) bioceramics are found to have better bone-bonding ability than pure HA in bony sites [6–8] and even show new bone formation within their porous structure in non-osseous tissues (certain bone-inducing phenomenon) [9–12]. It seems that the more similar the phase composition between calcium phosphate materials and bone apatite, the better the bioperformance of the materials in osseous environment.

However, unsintered natural bone gives, in fact, a mineral phase of non-stoichiometric apatite whose presence in bone is in the form of thin needle-like crystals (5–20 nm in diameter by 60 nm in length) with a poorly crystallized apatite structure and a Ca/P molar ratio between 1.67 and 1.5 [13–17]. Based on this, several methods have been used to prepare needle-like or fibrous non-stoichiometric apatite crystals which might be able to further improve the osteointegration [18–20]. But, so far, although studies on non-stoichiometric apatite have been carried out for many years, both in material science and in biomedical materials field [21–26], some properties are still unclear, such as whether water molecules are present in the crystal structure of non-stoichiometric apatite and whether the condensation of HPO_4^{2-} ions can occur over a wide temperature range more than 600 °C, as well as what is the relationship between the shape change and phase transition of non-stoichiometric apatite crystals? The nanometre-size needle-like non-stoichiometric apatite crystals made in our laboratory by hydrothermal processing provide a means for analysing and answering those questions posed above.

2. Materials and methods

Needle-like non-stoichiometric apatite crystals were prepared by hydrothermal treatment of fully washed as-prepared calcium phosphate precipitates at 140 °C under 0.3 MPa for 2 h. The precipitates were synthesized by dropping slowly an $(NH_4)_2HPO_4$ aqueous solution into a stirred $Ca(NO_3)_2$ aqueous solution according to a method similar to Jarcho *et al.* [27]. The pH value for both solutions was adjusted to 11 with ammonium solution and the reaction was set at room temperature.

These crystals were fired at 650 °C, 750 °C, 850 °C, 920 °C and 1100 °C for 1 h in ambient atmosphere, separately. The Ca/P molar ratio was measured with an atomic absorption spectrometer for calcium and an ultraviolet spectrophotometer for phosphorus. The shape change was observed by transmission electron microscopy (TEM), and the phase transition was tested through X-ray diffractometer (XRD) and infrared spectroscopy (IR).

3. Results

3.1. TEM photographs

Fig. 1 shows the TEM photographs of the starting needle-like crystals and those fired at 650 °C, 750 °C,

*To whom correspondence should be addressed.

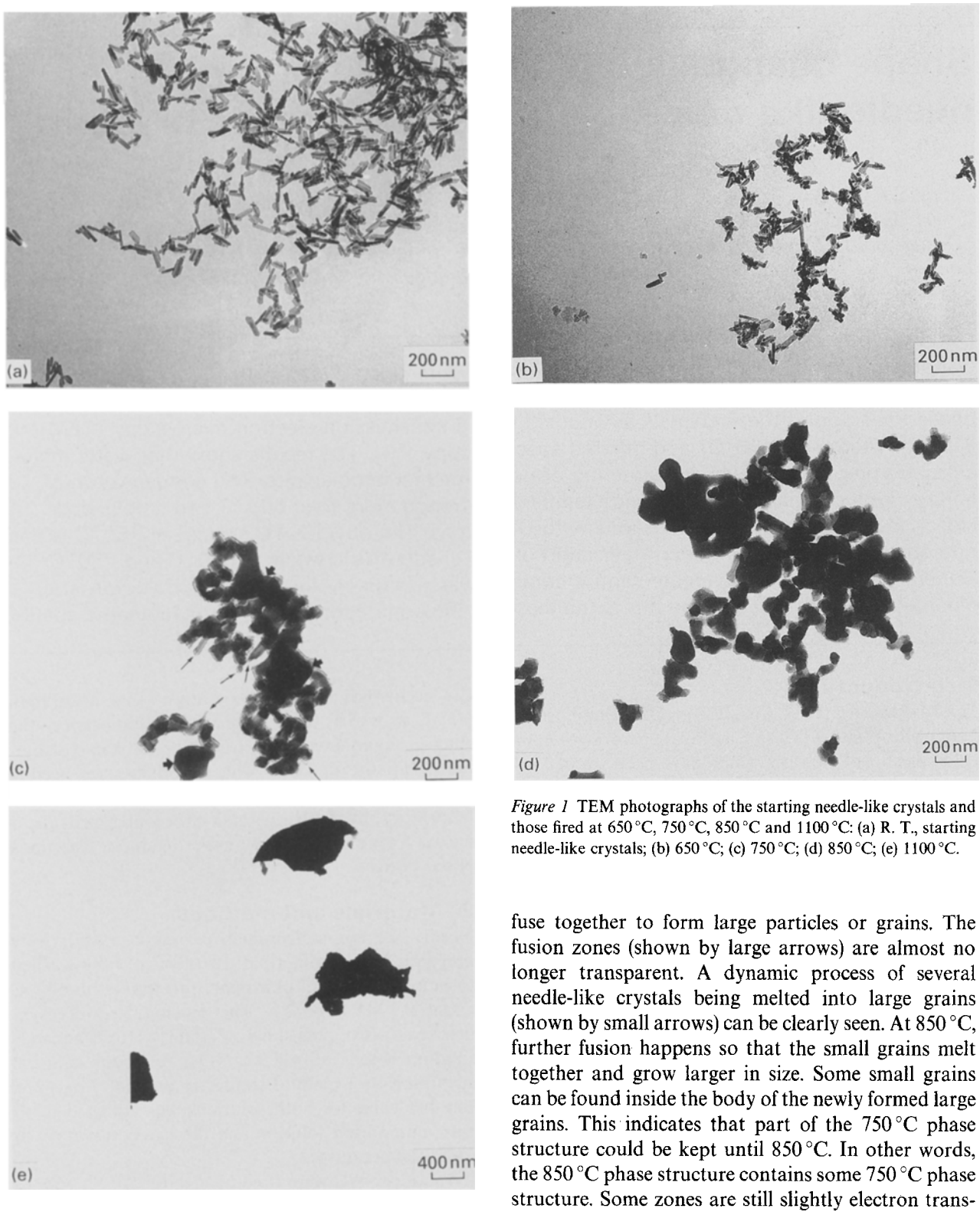

Figure 1 TEM photographs of the starting needle-like crystals and those fired at 650 °C, 750 °C, 850 °C and 1100 °C: (a) R. T., starting needle-like crystals; (b) 650 °C; (c) 750 °C; (d) 850 °C; (e) 1100 °C.

850 °C and 1100 °C, respectively. The starting needle-like crystals have a uniform and non-aggregated morphology with a mean size of about 23 nm by 91 nm and a Ca/P molar ratio of 1.52. These crystals are demonstrated to be single crystals with the typical hexagonal structure of $P6_3/m$ space group and are electron-transparent. After heating at 650 °C, these crystals become short in length and show a little aggregation. Their mean size falls to about 22 nm by 67 nm and the average crystal volume decreases by nearly 35% compared with that of the starting crystals. At 750 °C, the aggregated crystals are melted and fuse together to form large particles or grains. The fusion zones (shown by large arrows) are almost no longer transparent. A dynamic process of several needle-like crystals being melted into large grains (shown by small arrows) can be clearly seen. At 850 °C, further fusion happens so that the small grains melt together and grow larger in size. Some small grains can be found inside the body of the newly formed large grains. This indicates that part of the 750 °C phase structure could be kept until 850 °C. In other words, the 850 °C phase structure contains some 750 °C phase structure. Some zones are still slightly electron transparent. At 1100 °C, irregular fully crystallized electron-non-transparent ceramic particles are observed.

3.2. XRD patterns

The phase composition of the starting needle-like crystals and those fired at high temperatures are shown in Fig. 2. The starting crystals have a poor crystalline apatite structure. The 650 °C XRD pattern of those short crystals is similar to that of the starting crystals except a trace of TCP peak. At 750 °C, TCP phase increases obviously and results in a clear biphasic structure of HA and TCP, in which TCP content is nearly 29% of the total content. Unlike

other samples, sample (d-1) was drawn directly from the oven at 920 °C, while other samples were taken out at room temperature when the oven had cooled down. This sample exhibits a biphasic structure of about half HA and half TCP. Sample (d-2) shows more TCP component, nearly 70% of the total content. This indicates that the reaction is still in progress during the cooling process. The 1100 °C XRD pattern gives a structure consisting of approximate 87% TCP and 13% HA, which is consistent with the Ca/P molar ratio, 1.52, of the starting needle-like crystals. It is very clear that the content of TCP phase increases in succession with the increasing temperature.

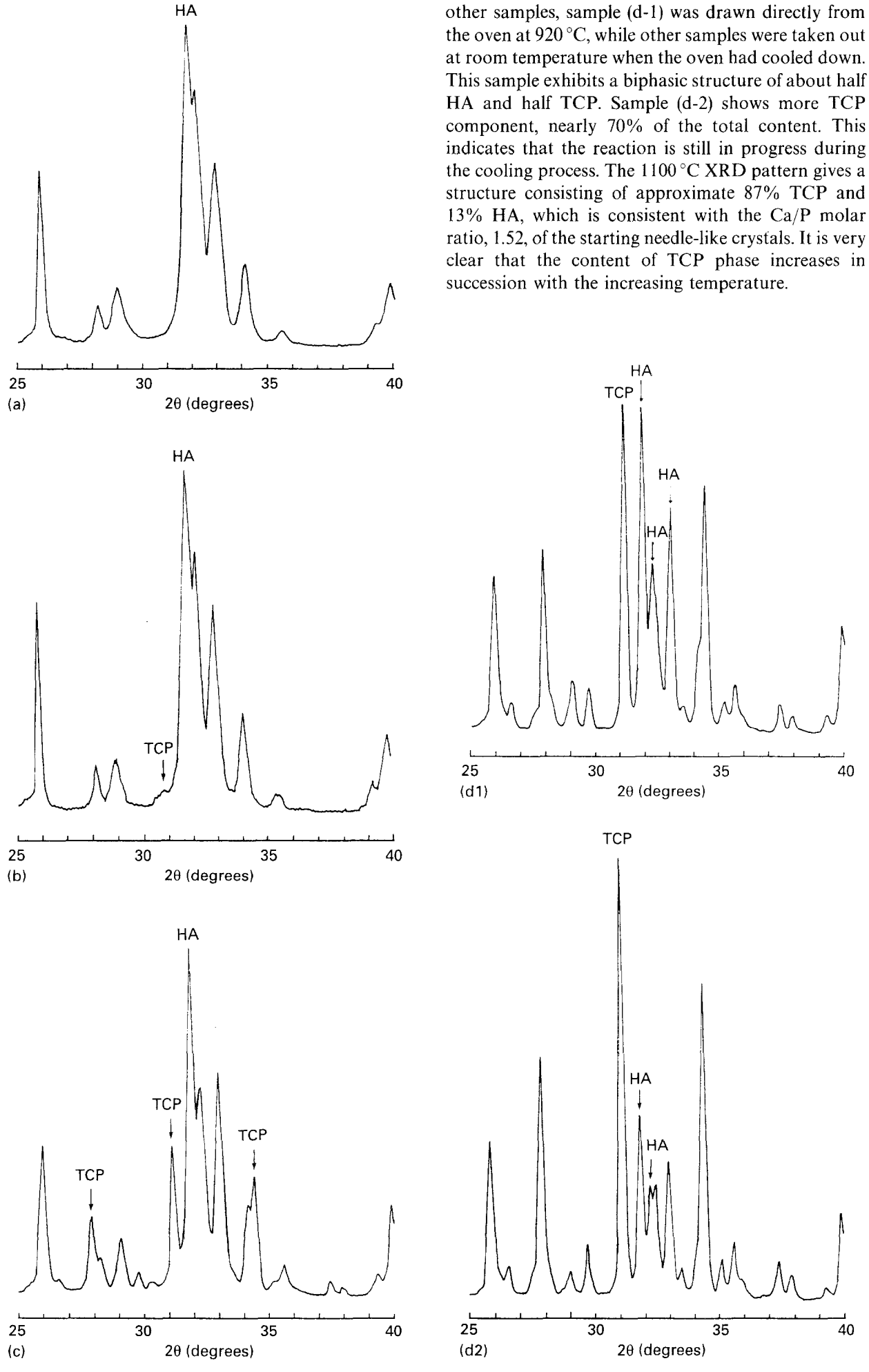

Figure 2 XRD patterns of the starting needle-like crystals and those fired at 650 °C, 750 °C, 920 °C and 1100 °C: (a) R. T., starting needle-like crystals; (b) 650 °C; (c) 750 °C; (d-1) drawn directly at 920 °C; (d-2) 920 °C; (e) 1100 °C.

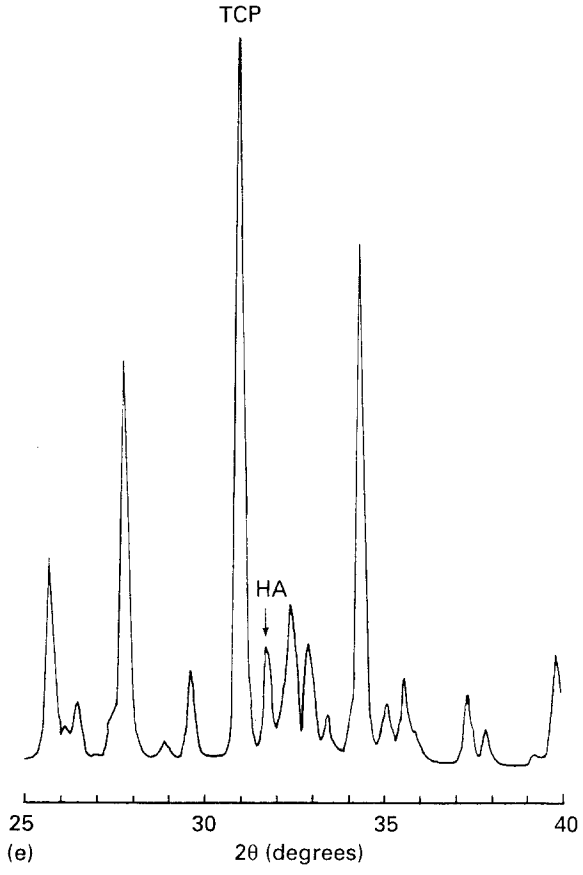

Figure 2 (Continued).

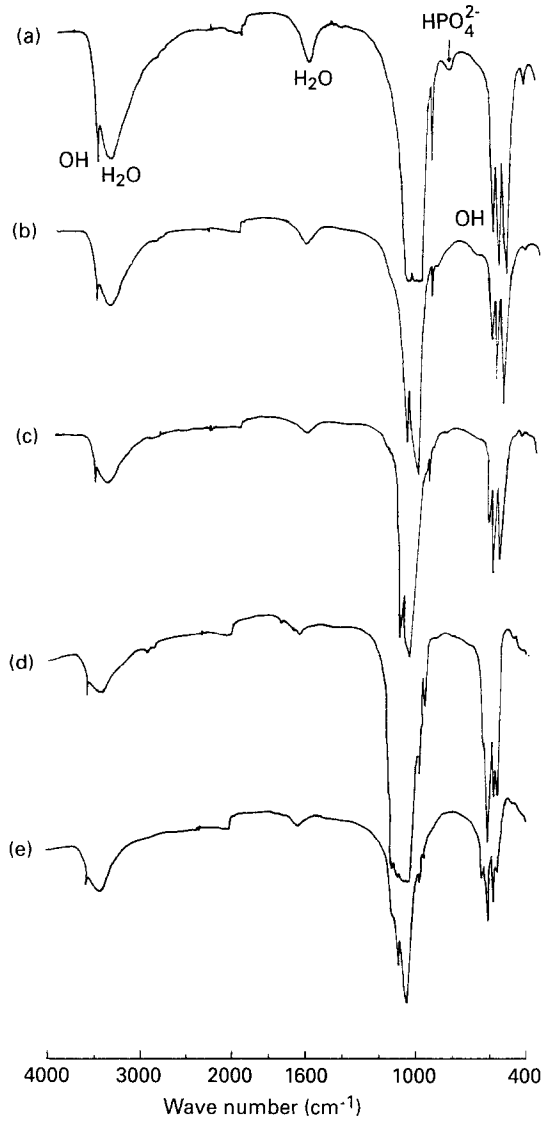

Figure 3 IR spectra of the starting needle-like crystals and those fired at 650 °C, 750 °C, 920 °C and 1100 °C: (a) R. T., starting needle-like crystals; (b) 650 °C; (c) 750 °C; (d) 920 °C; (e) 1100 °C.

3.3. IR spectra

The IR spectrum in Fig. 3a indicates the presence of OH^-, H_2O and HPO_4^{2-} as well as PO_4^{3-} in the starting apatite crystals. The peaks at 3571 and 633 cm^{-1} are due to OH^- ions [23, 28], the 875 cm^{-1} peak is caused by HPO_4^{2-} ions. The broad bands from 3700 to 2500 cm^{-1} and around 1635 cm^{-1} arise from water, and the other is due to PO_4^{3-} ions. It can be seen that the quantity of the OH^- decreases with the increasing temperature. The water content decreases a lot during heating to 650 °C, and seems unchanged after 750 °C. At 650 °C, a peak at 940 cm^{-1} corresponding to TCP phase appears, while the 875 cm^{-1} peak disappears. At 750 °C, the lost 875 cm^{-1} peak comes out again. The wide peak near 875 cm^{-1} at 920 °C IR spectrum could possibly represent the remaining small amount of HPO_4^{2-} ions at this moment. The IR spectrum at 1100 °C shows a TCP structure with small OH^- peaks (corresponding to a small amount of HA phase), which is also in agreement with the Ca/P molar ratio, 1.52, of the starting needle-like crystals.

4. Discussion

Apatite with a general formula $Ca_{10-x}(HPO_4)_x(PO_4)_{6-x}(OH)_{2-x}$ $(0 < x < 2)$ is called non-stoichiometric, or calcium deficient apatite which has an apatite or HA crystal structure and a Ca/P ratio between 1.67 and 1.33. The starting needle-like crystals in this experiment show clearly an apatite structure and a Ca/P ratio of 1.52. This indicates that these crystals are non-stoichiometric ones with a formula $Ca_{9.12}(HPO_4)_{0.88}(PO_4)_{5.12}(OH)_{1.12}$ ($x = 0.88$, identical to Ca/P ratio = 1.52). In Fig. 1, the whole process of the crystal shape change with increasing temperature can be observed. The 35% decrease of the average crystal volume at 650 °C and the fusion of the short and slightly aggregated crystals, starting from their contacted interface, and thus produced structure rearrangement or recrystallization during 650 °C to 750 °C are the most obvious and important phenomena. After 750 °C, the recrystallization is still in progress until 1100 °C, at which fully crystallized large ceramic particles are formed. In Fig. 2, phase transition can be clearly seen after 650 °C, and the higher the heating temperature, the higher the TCP content in the biphasic HA and TCP structure. Comparison of the TEM photographs and the XRD patterns leads us to the conclusions that the obvious TCP phase at 750 °C is the outcome of the fusion and recrystallization of the needle-like crystals during 650 °C and 750 °C; such fusion and recrystallization proceeds with increasing temperature above 750 °C. The two phase structures of HA and TCP can exist in the same grain. The non-stoichiometric apatite crystals, based on their

starting Ca/P molar ratio, change successively to TCP with the increasing temperature and finally to stoichiometric HA and TCP.

Perhaps one would ask what is the reason for the large decrease of the average crystal volume or relevant weight loss at 650 °C? The reason is, of course, the release of water, which could be from the condensation of HPO_4^{2-} ions before 650 °C, i.e., $2HPO_4^{2-} \rightarrow P_2O_7^{4-} + H_2O$, or directly from the lattice bound water. For the former, if the condensation of HPO_4^{2-} ions is finished before 650 °C, a great amount of $P_2O_7^{4-}$ ions will be produced corresponding to the 35% volume decrease. However, in the 650 °C and 750 °C XRD patterns, no $P_2O_7^{4-}$ peaks can be found. Furthermore, if the reaction of $P_2O_7^{4-}$ ion with OH^- ion, that is $P_2O_7^{4-} + 2OH^- \rightarrow 2PO_4^{3-} + H_2O$ happens immediately after the condensation of HPO_4^{2-} ions, it should produce a large amount of TCP phase at once. This is not in agreement with the successive increase of the TCP phase with increasing temperature as shown in Fig. 2. Especially in 650 °C XRD pattern, only a trace of TCP phase can be observed. Therefore, the large volume decrease of the needle-like crystals is caused by the direct release of lattice bound water. In other words, water molecules can exist in the crystal structure of non-stoichiometric apatite. On the other hand, the successive increase of the TCP phase above 650 °C is the result of the two reactions: the condensation of HPO_4^{2-} ions and the reaction of $P_2O_7^{4-}$ ion with OH^- ion, the latter happening closely after the former over a wide temperature range. Otherwise, $P_2O_7^{4-}$ peaks should be observed in XRD patterns in this temperature range.

The existence of HPO_4^{2-} ions can be seen not only from the IR spectrum of the starting needle-like crystals and the 750 °C IR spectrum, but also deduced from the XRD patterns. After 650 °C, when a part of TCP phase is formed, the XRD patterns give a biphasic structure consisting of HA and TCP in which the HA phase is still a non-stoichiometric one with a Ca/P ratio between 1.67 and 1.52. That is because the starting Ca/P ratio, 1.52, is a constant and cannot be changed in the whole temperature range. Thus, when a part of TCP phase with the lowest Ca/P ratio 1.50 appears, the Ca/P ratio of the residual HA phase in the biphasic structure will be more than 1.52 but less than 1.67. As a result of this, the fact that HPO_4^{2-} ions are present and the condensation of HPO_4^{2-} ions can happen at a temperature more than 650 °C are proven again.

Generally, the condensation of HPO_4^{2-} ions happens below 650 °C in $CaHPO_4$ material. Then, why in non-stoichiometric apatite can the same condensation occur at a higher temperature than 650 °C? In fact, in non-stoichiometric apatite, the HPO_4^{2-} ions are present within the apatite crystal lattice, not in the $CaHPO_4$ structure. In non-stoichiometric apatite $Ca_{10-x}(HPO_4)_x(PO_4)_{6-x}(OH)_{2-x}$ $(0 < x < 2)$, when $x = 1$, corresponding to a Ca/P ratio of 1.5 which is close to 1.52 of the sample used in this experiment, one unit cell of its crystal structure contains only one HPO_4^{2-} ion, in addition to nine Ca^{2+} ions, five PO_4^{3-} ions and one OH^- ion. Thus, the condensation of two HPO_4^{2-} ions from two different unit cells will be subjected to the restriction of the apatite crystal structure. That is to say, HPO_4^{2-} ions need greater energy (equivalent to higher temperature) to realize their condensation. Moreover, the condensation temperature and time will also depend on HPO_4^{2-} position in the apatite crystal structure.

The disappearance of the 875 cm^{-1} HPO_4^{2-} peak in the 650 °C IR spectrum does not mean the completion of condensation of HPO_4^{2-} ions before 650 °C, since the same peak can be clearly seen in the 750 °C IR spectrum. Some authors also found the presence of HPO_4^{2-} at 700 °C by chemical analysis [21] or in the IR spectrum [28]. The HPO_4^{2-} peak at 650 °C could be concealed by the crystal defects and the local disorder after the release of lattice bound water and before the fusion or recrystallization of the short crystals at 650 °C and 750 °C. At 750 °C, recrystallization makes the HPO_4^{2-} peak appear again. The decrease of the water peak in the 650 °C IR spectrum is mainly due to the release of the lattice bound water. The unchanged water absorption peaks above 750 °C in the IR spectra are due to the surface adsorbed water.

Viewing the whole process, we conclude that the nanometre-size needle-like crystals are very useful in understanding in detail the shape change and phase transition and their interrelation in non-stoichiometric apatite materials. Moreover, these needle-like crystals which contain water in their crystal structure will also be helpful to an understanding of the nature and properties of calcified tissues. Generally stoichiometric apatite cannot contain water in its crystal structure while non-stoichiometric apatite can. Maybe this is the reason why bone contains non-stoichiometric apatite. The lattice bound water could play an important role in bone growth and bone-bonding of biomaterials. The similarity between these crystals and bone apatite crystals provides an opportunity to build a bone-like implant composed of these needles and special organic matrixes (e.g. collagen) and cells.

Acknowledgements

The authors thank Mr Joop Wolke, Mrs Jolanda de Blieck and Mr Jurren Koerts for their assistance with the experiments. The authors are also grateful to the Commission of the European Communities for subsidizing this study.

References

1. K. DE GROOT, in "Bioceramics of calcium phosphate" (CRC Press, Bocca Raton, 1983).
2. L. L. HENCH and J. WILSON, *Science* **226** (1984) 630.
3. H. AOKI, in "Science and medical applications of hydroxyapatite" (JAAS Press, Japan, 1991).
4. P. DUCHEYNE, *J. Biomed. Mater. Res.* **21** (A2) (1987) 219.
5. W. BONFIELD, M. D. GRYNPAS, A. E. TULLY, J. BOWMAN and J. ABRAM, *Biomaterials* **2** (1985) 85.
6. P. FRAYSSINET, J. L. TROUILLET, N. ROUQUET, E. AZIMUS and A. AUTEFAGE, *ibid.* **14** (1993) 423.
7. G. DACULSI, N. PASSUTI, S. MARTIN, C. DEUDON, R. Z. LEGEROS and RAHER, *J. Biomed. Mater. Res.* **24** (1990) 379.

8. M. KOHRI, K. MIKI, D. E. WAITE, H. NAKAJIMA and T. OKABE, *Biomaterials* **14** (1993) 299.
9. LI YUBAO, ZHANG XINGDONG, CHEN WEIQUN, LIU YUHUA, C. P. A. T. KLEIN and K. DE GROOT, in Transactions of the 19th Annual Meeting in Conjunction with the 25th International Biomaterials Symposium, Birmingham, April, 1993 (Society For Biomaterials, Minneapolis, USA, 1993) p. 165.
10. ZHANG XINGDONG, LI YUBAO, ZHOU PING, WU CONG and WANG MUTANG, in "Advanced prosthodontics worldwide", edited by H. Trusu (WCP' 91, Hiroshima, 1991), p. 578.
11. H. YAMASAKI and H. SAKAI, *Biomaterials* **13** (1992) 308.
12. J. M. TOTH, K. L. LYNCH and K. R. HAMSON, in Transactions of the 4th World Biomaterials Congress (Berlin, April, 1992) p. 65.
13. J. L. KATZ and R. A. HARPER, in "Encyclopedia of materials science and engineering" (Pergamon, Oxford, 1986), p. 475.
14. J. B. PARK and R. S. LAKES, in "Biomaterials: an introduction" (Plenum Press, New York and London, 1992) 192.
15. A. S. POSNER, *Physiol. Rev.* **49** (1969) 760.
16. *Idem., Clin. Orth. and Relat. Res.* **200** (1985) 87.
17. R. M. BILTZ and E. D. PELLEGRINO, *J. Dent. Res.* **62** (1983) 1190.
18. K. IOKU and M. YOSHIMURA, *Phosphorus Research Bulletin* **1** (1991) 15.
19. M. TANAHASHI, K. KAMIYA, T. SUZUKI and H. NASU, *J. Mater. Sci. Mater. Med.* **3** (1992) 48.
20. E. C. KREIDLER and F. A. HUMMEL, *Am. Mineral* **55** (1970) 170.
21. E. E. BERRY, *J. Inorg. Nucl. Chem.* **29** (1967) 317.
22. Idem., *ibid.* **29** (1967) 1585.
23. J. ARENDS, J. CHRISTOFFERSEN, M. R. CHRISTOFFERSEN, H. ECKERT, B. O. FOWLER, J. C. HEUGHEBAERT, G. H. NANCOLLAS, J. P. YESINOWSKI and S. J. ZAWACKI, *J. Cryst. Growth* **84** (1987) 515.
24. A. MORTIER, J. LEMAITRE, L. RODRIQUE and P. G. ROUXHET, *J. Solid State Chem.* **78** (1989) 215.
25. G. MONTEL, G. BONEL, J. C. HEUGHEBAERT, J. C. TROMBE and C. REY, *J. Cryst. Growth* **53** (1981) 74.
26. J. L. LACOUT, in "Biomaterials-hard tissue repair and replacement", edited by D. Muster (Elsevier Science Publishers B. V., 1992), p. 81.
27. M. JARCHO, C. H. BOLEN, M. B. THOMAS, J. BOBICK, J. F. KAY and R. H. DOREMUS, *J. Mater. Sci.* **11** (1976) 2027.
28. JIMING ZHOU, XINGDONG ZHANG, JIYONG CHEN, SHAOXIAN ZENG and K. DE GROOT, *J. Mater. Sci. Mater. Med.* **4** (1993) 83.

Received 11 June
and accepted 10 September 1993